Methods and Applications in Fluorescence

TECHNICAL NOTE

A-TEEM^{TM}, a new molecular fingerprinting technique: simultaneous absorbance-transmission and fluorescence excitation-emission matrix method

RECEIVED
26 October 2017

REVISED
20 December 2017

ACCEPTED FOR PUBLICATION
16 January 2018

PUBLISHED
5 February 2018

Alessia Quatela[1], **Adam M Gilmore**[2], **Karen E Steege Gall**[2], **Marinella Sandros**[2], **Karoly Csatorday**[2], **Alex Siemiarczuk**[2], **Boqian (Ben) Yang**[2] **and Loïc Camenen**[1]

[1] Horiba Scientific, Avenue de la Vauve, Passage Jobin Yvon CS 45002, F-91120 Palaiseau, France
[2] Horiba Scientific, 3880 Park Avenue Edison, NJ 08820, United States of America

E-mail: alessia.quatela@horiba.com

Keywords: EEM, inner-filter effects, PARAFAC, water quality, wine analysis, proteins, insulin

Abstract

We investigate the new simultaneous absorbance-transmission and fluorescence excitation-emission matrix method for rapid and effective characterization of the varying components from a mixture. The absorbance-transmission and fluorescence excitation-emission matrix method uniquely facilitates correction of fluorescence inner-filter effects to yield quantitative fluorescence spectral information that is largely independent of component concentration. This is significant because it allows one to effectively monitor quantitative component changes using multivariate methods and to generate and evaluate spectral libraries. We present the use of this novel instrument in different fields: i.e. tracking changes in complex mixtures including natural water, wine as well as monitoring stability and aggregation of hormones for biotherapeutics.

Introduction

It is well known that fluorescence spectra are subject to significant and predictable distortions caused by concentration-dependent inner filter effects (IFE) and it is the user's responsibility to evaluate the absorbance values versus concentration of the sample to ascertain the Beer–Lambert linearity requirement [1]. The Primary inner-filter effect (PIF) occurs when excitation light is absorbed by components in the sample before it reaches the area of intersection of the excitation and emission beam paths where fluorescence can be excited and hence detected. The secondary inner-filter effect (SIF) occurs when the fluorescence emitted in the intersected regions of the excitation and emission beam paths is absorbed by sample components before it can exit the cell to reach the emission detector. Both SIF and PIF can be caused by sample components that absorb light independently of whether these components fluorescence. These effects are always present at any OD value in the overlapping absorbance and fluorescence emission regions [2].

The literature cites many studies of the IFE corrections, all of which relate to formulating and testing equations [3] dealing with the optical extinction coefficients, cell path lengths, cell positions, and beam geometry as the latter are defined by the focal properties (f-numbers) of the excitation and emission beam paths. In practice one normally measures the absorbance spectrum of the sample where this overlaps the fluorescence excitation and/or emission spectral regions of interest. Ideally this is done simultaneously with the fluorescence measurements in the same cell and instrument to minimize differences due to geometry or the state of the sample.

Here we present a new method for simultaneously generating the individual excitation and emission spectra for all fluorescent sample components while also providing information on components that absorbed light but did not fluoresce as well as information needed to correct the fluorescence spectra for the sample concentration-dependent IFE as already described [2].

Instrumentation

This study employs the method of simultaneous absorbance-transmission and fluorescence excitation-emission matrix (A-TEEM^{TM}) spectroscopy with the

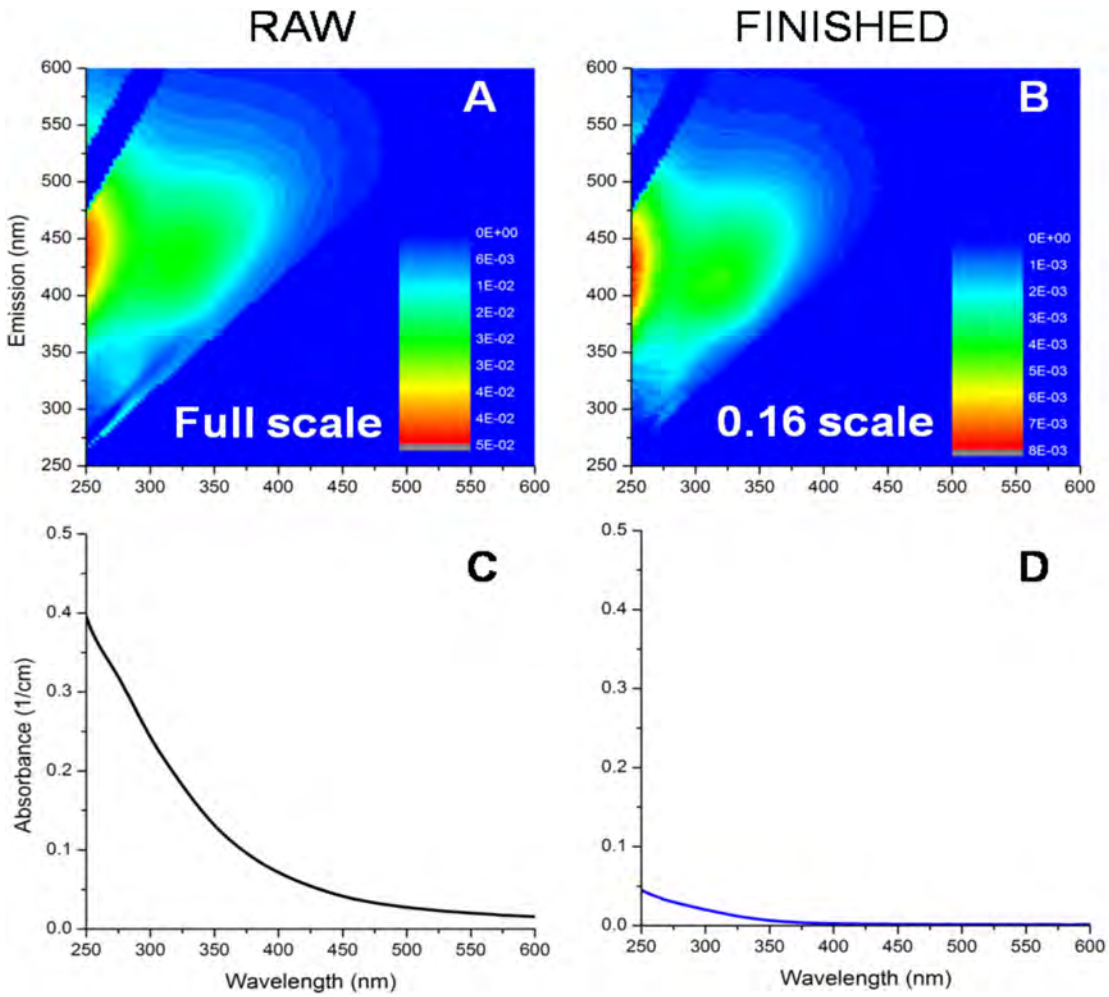

Figure 1. Comparison of typical Aqualog® EEMs (top) and UV–vis absorbance spectra (bottom) for corresponding raw (left) and finished (right) water samples measured on the same day. Absorbance units per cm are reported.

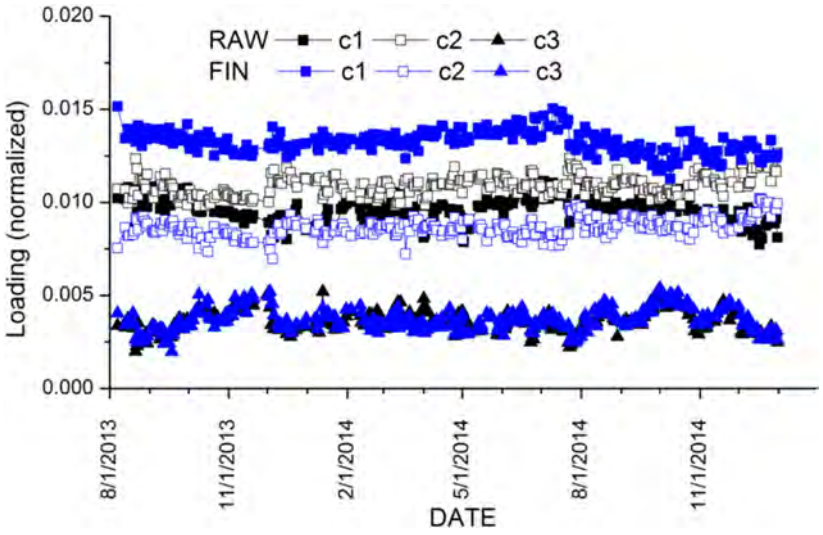

Figure 2. Normalized concentration PARAFAC loadings for c1, c2 and c3 for the daily raw (RAW) and finished (FIN) samples.

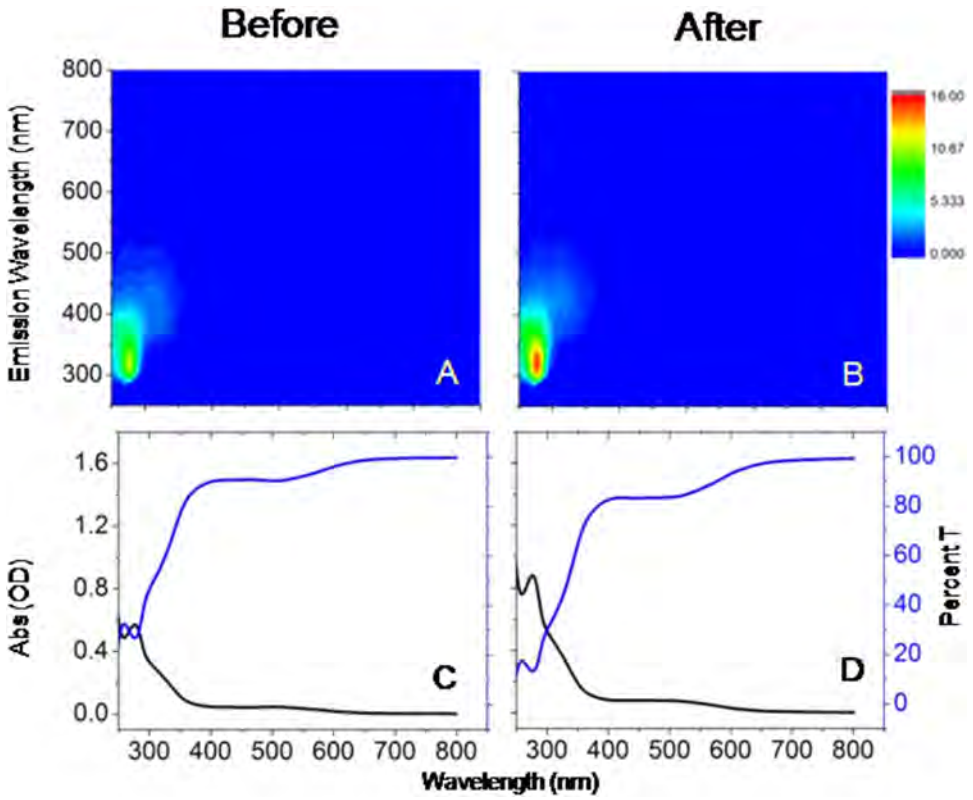

Figure 3. Fluorescence EEMs (A) and (B) and corresponding (C) and (D) absorbance (black lines) and %transmittance (blue lines) spectra for the Italy wine sample Before (A) and (C) and After (B) and (D) a one week oxidation treatment.

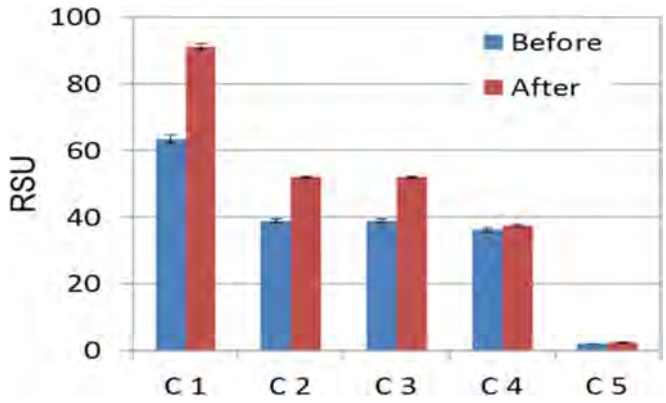

Figure 4. Comparison of the five PARAFAC component scores in the Italy wine samples ($n = 3$ replicates per sample) before and after oxidation. Component scores are reported normalized water Raman scattering units (RSU).

dedicated patented Aqualog® from Horiba Instruments Inc. [1].

The Aqualog® optical bench includes a special aberration-corrected double-grating excitation monochromator, a reference detector and absorbance detector (both Si photodiodes), and a unique emission detector comprised of a thermoelectrically cooled back-illuminated CCD and spectrograph. The system incrementally scans excitation from high energy to low energy and can collect the full emission spectrum at each excitation increment to rapidly and simultaneously generate absorbance spectra and fully corrected excitation-emission spectral maps or matrices.

The Aqualog®-coupled software is equipped with a built-in tool for normalization to water Raman scattering or quinine sulfate units for the defined emission conditions, correction for the influence of IFE and Rayleigh masking. The analysis of the fully corrected EEM data involves the Aqualog® Datastream package based on the multivariate routine known as PARAFAC (Solo + MIA package from Eigenvector Research Inc.).

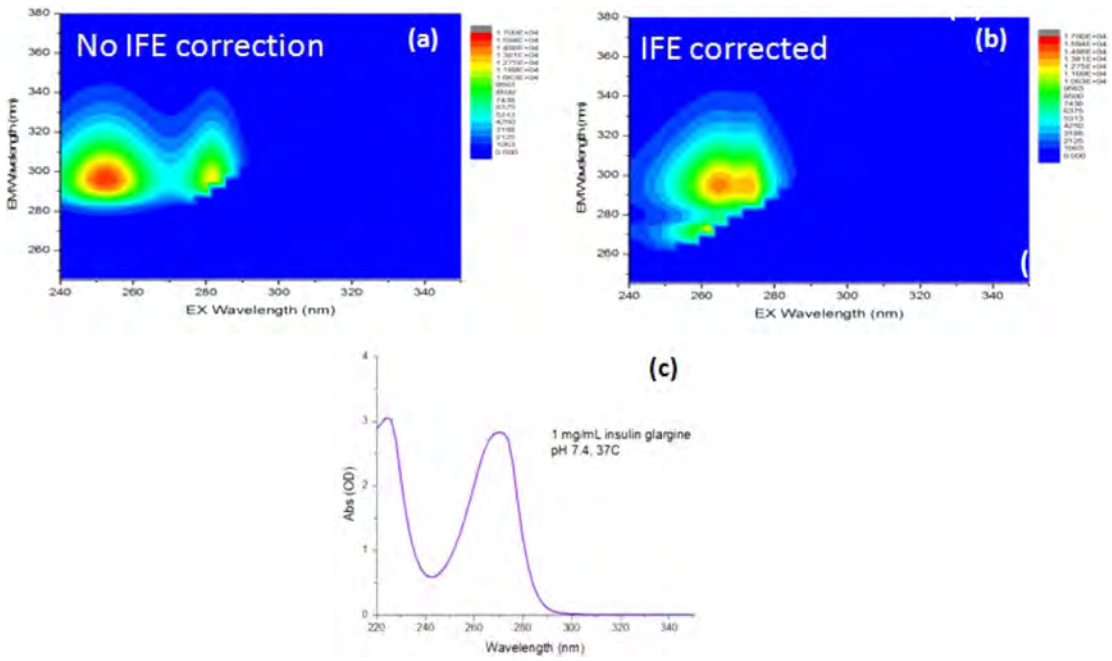

Figure 5. EEM (a), (b) and absorbance (c) data of commercial formulation insulin pH 7.4, Temp = 37 °C.

Table 1. Quantitative assignment of PARAFAC components.

PARAFAC component	Excitation max (nm)	Emission max (nm)	Name
C1	278	340	Caffeic acid
C2	263	380	Flavonol like
C3	280	300	Epicatechin
C4	315	405	Gentisic acid
C5	445	568	Anthocyanin

Current applications

Water quality

Drinking water treatment plants that primarily use surface water sources are regulated because certain water components are precursors to toxic disinfection by-products (DBPs) that may react over time in the distribution system with halogenated disinfectants. These components, namely total dissolved organic carbon (TOC), are commonly subject to significant variations in often unpredictable patterns associated with rainfall, snow-melt and other events that influence sporadic drainage of organic materials into the source water.

The Aqualog® was used to monitor dissolved organic matter pertaining to EPA Stage 2 disinfection by-product rule (DBPR2) compliance [4] in a typical surface water source drinking water treatment plant.

Duplicate daily raw source and finished water samples were filtered (0.45 μm) immediately before analysis. All samples were equilibrated to room temperature (25 °C) nominally prior to analysis. The Aqualog® EEM and absorbance measuring conditions included an excitation/absorbance range from 250 to 600 nm using 3 nm for excitation intervals and 3.28 nm for emission using a medium gain and 2 s integration for emission detection. The blank sample for emission and absorbance was a sealed TOC-free water sample (Starna 3Q-10) from Starna Scientific Inc. All 3.5 ml samples were analyzed using 1 cm path length suprasil 4-way clear fluorescence quartz cuvettes.

Figure 1 compares typical EEM and absorbance profiles for raw and finished water samples measured in the same daily sample set. The EEM data for the raw water exhibited around a 6.25 fold higher peak intensity than the finished water along with a broader and significantly red-shifted main emission band. The absorbance for the raw water also exhibited higher extinction at all wavelengths compared to the corresponding finished water sample.

To evaluate the quantitative changes in the EEMs associated with the treatment PARAFAC analysis was applied to all samples to decompose the excitation spectra, emission spectra and concentration loadings for the main fluorescent components. Three main components have been identified, mainly Component 1 (c1) identified as a humic/fulvic component with relatively lower molecular weight and aromaticity, Component 2 (c2), identified as a humic/fulvic component with higher molecular weight and aromaticity and Component 3 (c3) identified as a protein-like component.

Figure 2 compares the normalized PARAFAC concentration loadings for the three components for the daily raw and finished water samples. In the raw water, the main component was consistently Component 2

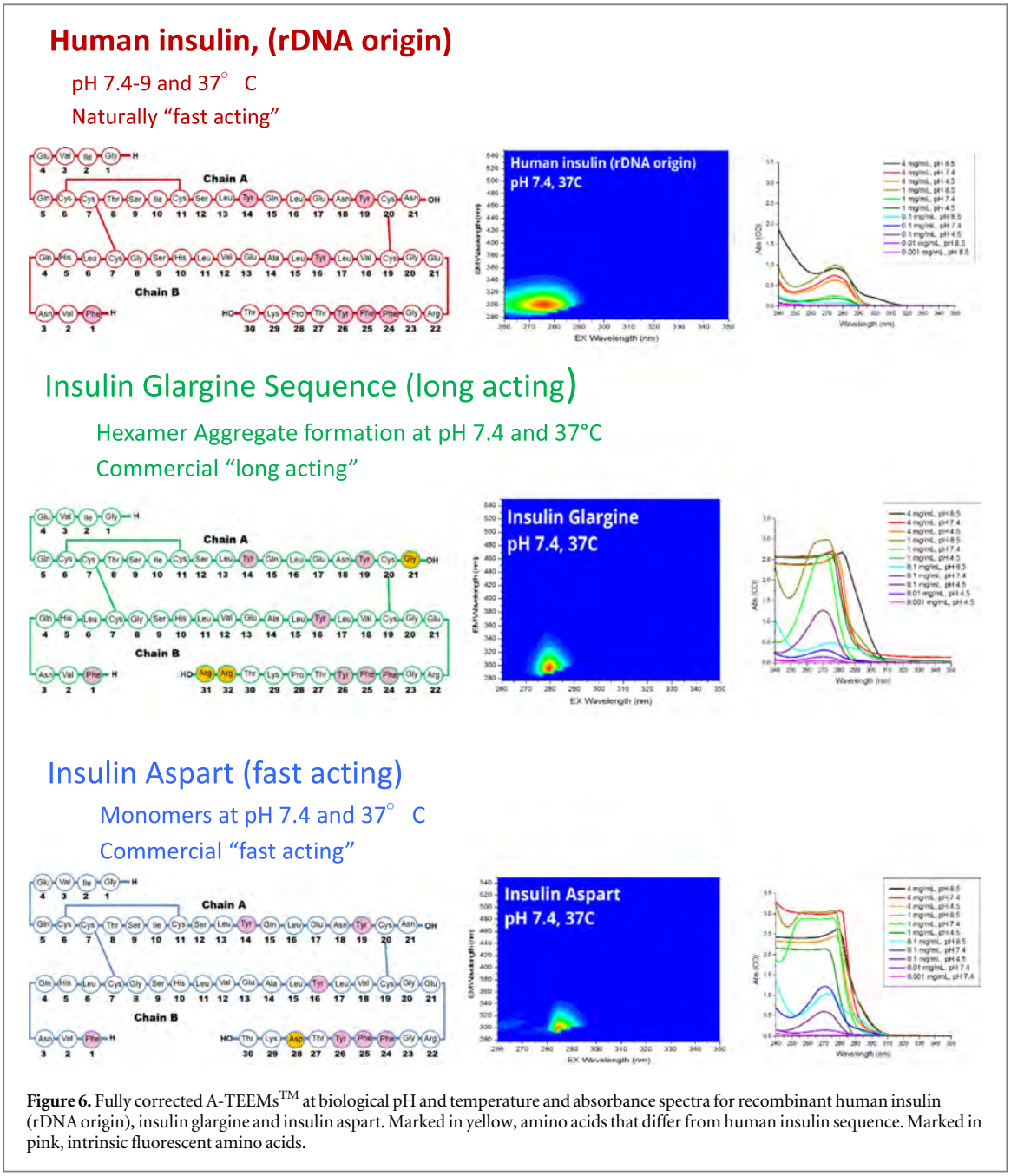

Figure 6. Fully corrected A-TEEMs^{TM} at biological pH and temperature and absorbance spectra for recombinant human insulin (rDNA origin), insulin glargine and insulin aspart. Marked in yellow, amino acids that differ from human insulin sequence. Marked in pink, intrinsic fluorescent amino acids.

whereas in the finished water, Component 1 dominated. The relative concentration of Component 3 remained largely unchanged between the treatments. The enhanced removal of Component 2 is consistent with the expected effects of coagulation to remove higher molecular weight organics more effectively than lower molecular weight species. Hence this pattern clearly correlated with the broader, red-shifted spectra for the main EEM bands in the raw water compared to the finished water shown in figure 1.

Wine analysis

Red wines contain several colored and fluorescent components, mostly polyphenolic in nature, which determine various quality parameters, including color and flavor [5]. Fluorescence and UV–vis spectroscopy have the potential to detect and resolve these components to effectively characterize unique compositional properties of red wines. Together the absorbance, transmission and fluorescence EEM data can be used to evaluate lot-to-lot, regional, and varietal characteristics, as well as sense the effects of aging, oxidation and sulfite treatment.

Figure 3 shows simultaneously recorded EEMs (A) and (B) and Absorbance and percent transmission spectra (C) and (D) for a typical Italian red wine from a freshly opened bottle Before (A) and (C) and After a one week exposure to air (B and D). The Aqualog® EEM and Absorbance measuring conditions included an excitation/absorbance range from 200 to 800 nm with a 3 nm increment and an emission range of 250–800 nm with a 4.65 nm CCD bin increment at medium gain and 0.1 s integration time.

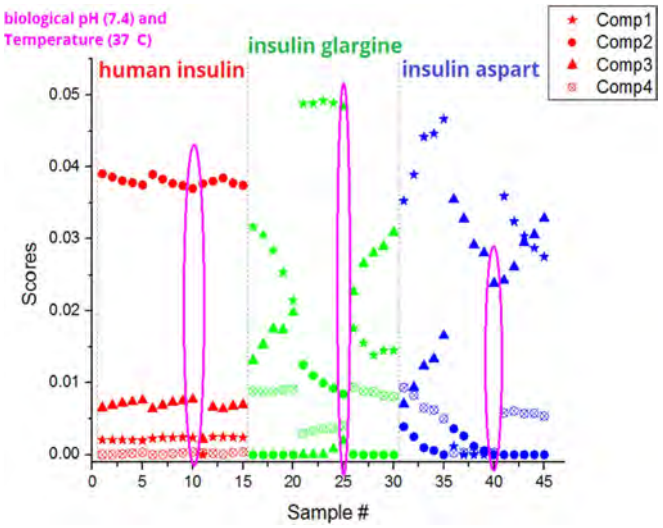

Figure 7. Component EEMs from PARAFAC multivariate chemometric analysis for the three types of insulin at commercial formulations (4 mg ml^{-1} insulin concentration). Circled in PINK are all data points measured at pH 7.4 °C and 37 °C.

The complex EEMs clearly exhibit the major contours in the UV excitation-emission range with the major excitation/emission peak around 275/309 nm. For both the Before and After samples the absorbance (and transmission) spectra exhibited a major extinction peak around 275 nm, a smaller shoulder peak around 320 nm and a second minor peak around 520 nm. The 275 nm peak region is commonly associated, at least in part, with phenolic compounds and the 520 nm peak region is generally associated with anthocyanin compounds [6]. Compared to the Before sample (C) the After sample (D) exhibited increased extinction across the entire absorbance spectrum associated with the oxidation phenomenon.

The complexity of the EEM spectral contours, which comprises multiple overlapping excitation and emission components, limits qualitative and quantitative visual interpretation to major contour elements. Hence, multivariate analysis is generally applied to decompose the EEM components in terms of quality and quantity.

The PARAFAC model evaluated in this study was constrained to yield non-negative values for all loading and score parameters. Table 1 reports the five spectral loading components resolved in the PARAFAC model developed using all the fresh and oxidized wine sample replicates. The components were compared to literature values for tentative identification [7].

Figure 4 compares the effects of oxidation on each of the PARAFAC components for the Italy wine sample. Component 1 was the dominant component before and after oxidation. While all five components increased significantly in intensity loading after oxidation, the deeper UV emitting components 1–3 increased relatively more than the longer emission wavelength components 4 and 5.

Insulin structure and analysis

Insulin is a protein-hormone, produced by the pancreas and is necessary for basic metabolic processes [8, 9]. The different types of commercial insulin therapeutics generally fall into two categories: fast-acting and long-acting insulin. The difference between short-acting and long-acting insulin is as little as between one and three residues in the protein sequence. These small sequence changes, along with controlled pH of storage and delivery, is used to either trigger or prevent the formation of insulin dimers and hexamers in the blood stream. The formation of these aggregates lets the body absorb insulin more slowly and the absence of aggregates makes it absorb more quickly. Changes in protein stability and structure, such as those important to the pharmacokinetics of insulin, are often measured using fluorescence emission spectra, UV–vis absorbance spectra or sometimes both, using intrinsically fluorescent amino acids.

Because commercial insulin formulations are of high concentration (4 mg ml^{-1}), the IFE correction is very important for measuring the A-TEEM^{TM} fingerprint (figure 5).

Three different insulin proteins have been analyzed at different concentrations, pH (4.5–8.5) and temperatures (5 °C–37 °C): recombinant human insulin [10], insulin-aspart (commercially available, fast acting), and insulin-glargine (commercially available, long-acting) as shown in figure 6.

PARAFAC analysis of intrinsic fluorescence A-TEEMs^{TM} has been performed in order to characterize the aggregation state of the different types of insulin. Four components have been identified in the commercial formulations: Components 1, 2 and 3 (Comp1, Comp2 and Comp3) identified as Tyrosine [11] and Component 4 (Comp4) identified as m-cresol [12], a preservative in insulin formulations (figure 7).

The red data points in figure 7 show the scores for a four-component PARAFAC model as fit to recombinant human insulin solutions at pH 4.5 (first five data points), pH 7.4 (2nd five data points) and pH 8.5 (last five data points). Each of the five repeats is at temperatures 5 °C, 20 °C, 25 °C, 30 °C, and 37 °C in that order. The models were repeated and plotted for insulin glargine (green data) and insulin aspart (blue data) in figure 7 under the same sequential conditions.

Insulin glargine, which is sequenced to produce aggregates at biological pH and temperature, shows a much larger score for component 1 (stars), which may be attributed to the blue-shifted spectrum of tyrosine when insulin is in aggregate form. Solutions of human insulin and insulin aspart, which are less likely to aggregate under the same conditions, show much lower scores for the same component 1.

It is evident that insulin sequences that vary by only 1–3 amino acids can be differentiated by intrinsic fluorescence A-TEEMs^{TM}. Commercial formulations of insulin have high concentrations and absorbance values, making the A-TEEM^{TM} method a good way to characterize such commercial protein therapeutic formulations where traditional fluorescence methods may fail. While this study is not giving any new information about insulin and how these proteins aggregate or not according to the formulation conditions, it does show that the A-TEEM^{TM} method can be used to characterize protein therapeutic formulations for aggregation behavior, even under conditions where there are only small differences in protein sequence. EEM has already shown great biology significance [13–18]; furthermore the A-TEEM^{TM} fingerprinting technique could potentially be used for other protein therapeutics such as vaccines, enzymes, inhibitors, and antibodies.

Conclusion

Fluorescence is recognized as a highly sensitive tool for the characterization of any kind of samples, but combined with other measurement techniques, it becomes even more powerful.

The A-TEEM^{TM} method as implemented in the patented Aqualog® is the only instrument of its kind that performs real-time simultaneous inner filter correction of fluorescence spectra to provide true, NIST-traceable, molecular fingerprints. This quality is essential for absolute and reproducible libraries of molecular fingerprints that can be relied on for credible quantitative analysis of a wide range of important substances.

The A-TEEM^{TM} method, combined with the Aqualog® spectrofluorometer, has been used to monitor the treatment of raw water providing a fast, accurate and easy to use tool. Its application has been extended into different areas like the wine study where it demonstrates the possibility to characterize the main compounds of the wine and also the level of oxidation.

The field of use of this multimodal methodology is huge: food industry, chemistry, petrochemicals and biomedical. In particular, the A-TEEM^{TM} reveals to be an extremely powerful method for the discrimination of the different type of existing insulins.

ORCID iDs

Alessia Quatela https://orcid.org/0000-0002-7224-9732

References

[1] Gilmore A M 2011 Water quality measurements with the Aqualog®. Spectroscopyonline.com
[2] Gilmore A M 2014 How to collect National Institute of Standards and Technology (NIST) traceable fluorescence excitation and emission spectra *Fluorescence Spectroscopy and Microscopy (Methods and Protocols)* (*Methods in Molecular Biology* vol 1076) ed Y Engelborghs and A Visser (Totowa, NJ: Humana Press)
[3] MacDonald B C, Lvin S J and Patterson H 1997 Correction of fluorescence inner filter effects and the partitioning of pyrene to dissolved organic carbon *Anal. Chim. Acta* **338** 155–62
[4] OFFICE OF WATER 2010 Comprehensive Disinfectants and Disinfection Byproducts Rules (Stage 1 and Stage 2): Quick Reference Guide. USEPA; http://water.epa.gov/drink
[5] Giovinazzo G and Grieco F 2015 Functional properties of grape and wine polyphenols *Plant Foods Hum. Nutrition* **70** 454–62
[6] Agati G, Matteini P, Oliveira J, de Freitas V and Mateus N 2013 Fluorescence approach for measuring anthocyanins and derived pigments in red wine *J. Agric. Food Chem.* **61** 10156–62
[7] Airada-Rodriguez D, Duran-Meras I, Galeno-Diaz T and Petter Wold J 2011 Front-face fluorescence spectroscopy: a new tool for control in the wine industry *J. Food Compos. Anal.* **24** 257–64
[8] Bi R C, Dauter A, Dodson E J, Dodson G G, Giordano F and Reynolds C D 1984 Insulin's structure as a modified and monomeric monomer *Biopolymers* **23** 391–5
[9] Blundell T L, Dodson G G, Hodgkin D C and Mercola D A 1972 Insulin: the structure in the crystal and its reflection in chemistry and biology *Adv. Protein. Chem.* **26** 379–402
[10] Larkins R G 1983 Human insulin *Aust. N.Z. J. Med.* **13** 647–51
[11] Ellis L, Tavaré J M and Levine B A 1991 Insulin receptor tyrosine kinase structure and function *Biochem. Soc. Trans.* **19** 426–32
[12] Van Faassen I, Verweij-van Vught A M, Lomecky-Janousek M Z, Razenberg P P and van der Veen E A 1990 Preservatives in insulin preparations impair leukocyte function. *In vitro* study *Diabetes Care* **13** 71–4
[13] Leiner M, Schaur R J, Wolfbeis O S and Tillian H M 1983 Visible fluorescence topograms of rat sera, and cluster analysis of fluorescence parameters of sera of yoshida ascites hepatoma-bearing rats *IRCS Med. Sci.* **11** 841–2
[14] Wolfbeis O S and Leiner M 1984 Characterization of edible oils via fluorescence topography *Microchim. Acta* **82** 221–33
[15] Wolfbeis O S and Leiner M 1985 Mapping of the total fluorescence of human blood serum as a new method for its characterization *Anal. Chim. Acta* **167** 203–15
[16] Koller E, Quehenberger O, Jürgens G, Wolfbeis O S and Esterbauer H 1986 Investigation of human plasma low density lipoprotein by three-dimensional fluorescence spectroscopy *FEBS Lett.* **198** 229–34
[17] Leiner M, Schaur R J, Wolfbeis O S and Desoye G 1986 Characteristic deviations of tryptophan fluorescence in sera of patients with gynecological tumors *Clin. Chem.* **32** 1974–8
[18] Leiner M J P, Hubmann M R and Wolfbeis O S 1987 The total fluorescence of human urine *Anal. Chim. Acta* **198** 13–23